First Neutron Star Redshift Measurement

- Overview of Possible Mechanisms for Accreting Neutron Stars.
- Summary of First Announced Measurement; Nature, Fall '02
  [Cottam, Paerels & Mendez, 2002 Nature, 420, 51]
- Our initial work on Fe Abundances & Spallation
  [Bildsten, Chang & Paerels, 2003, ApJ, July 1 '03
- Future Obs?

Spectral Lines from Neutron Stars

Challenge is to produce either an atomic or nuclear spectral line of known λ $\Rightarrow$ then identify with confidence ! $z = \frac{\Delta\lambda}{\lambda}$!

- Nuclear Emission (Shvartsman) of either ^{12}C, ^{16}O.. or $n + p \rightarrow D + \gamma$ (2.2 MeV)
  (Bildsten, Salpeter & Wasserman '92, '94)
- Atomic Lines, say from high Z,

$$E_{bind} = -9.2\,\text{kev}\left(\frac{Z}{26}\right)^2$$

Spallation Scenario

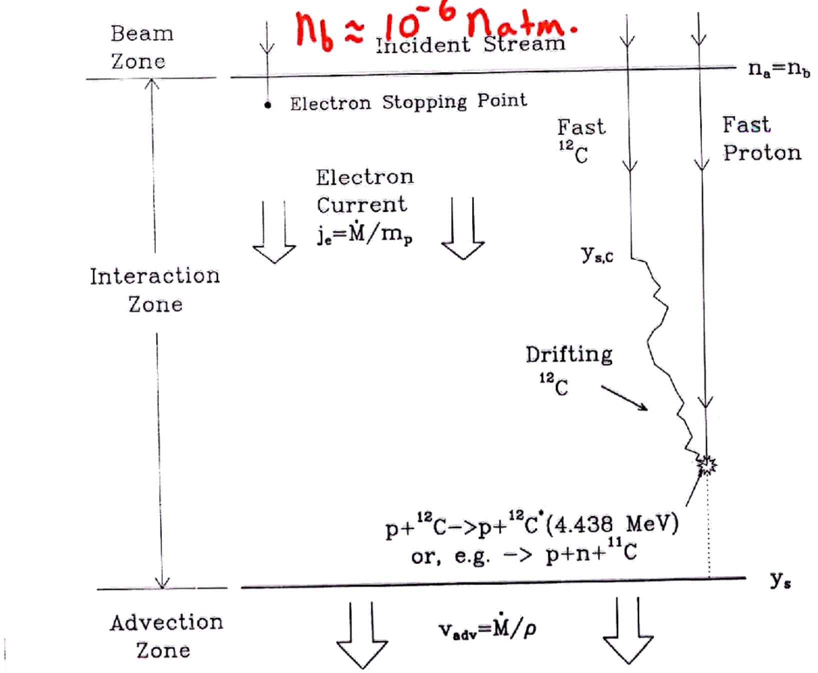

BSW '92

Coulomb Drag on e^- in atmos., stops incident beam and

$$y_{stop} = \frac{1}{\sigma_T}\frac{m_p}{6m_e}\frac{1}{\ln\Lambda}\left(\frac{v_i}{c}\right)^4\frac{A}{Z^2}$$

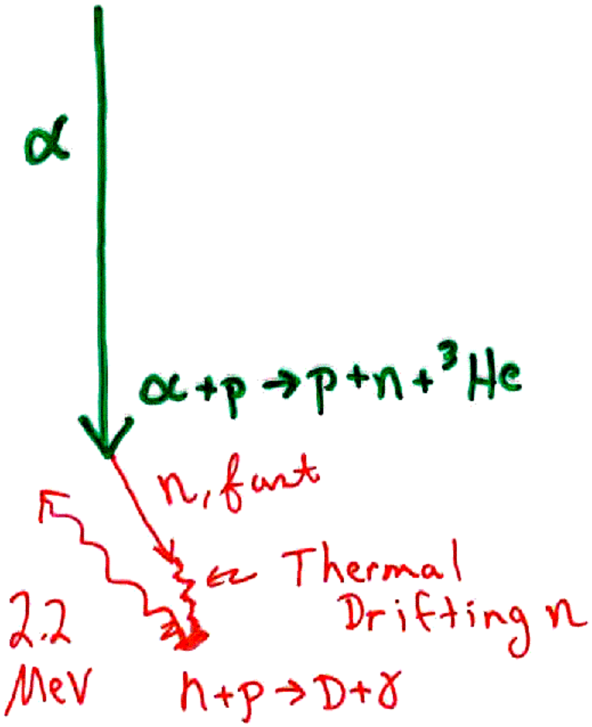

; '94

Gamma-Ray Punchlines

(BSW '92; '94)

- For accreting NSs with cosmic abundances, expected line emission from C, O
  $\Rightarrow$ 10-100 times too faint for Integral
- However the spalled ^{4}He liberates $n \Rightarrow$ 2.2 MeV line at levels which can be probed by INTEGRAL Looking right Now.

Atomic Lines

Challenge for large atomic features from a NS photosphere is Ionization balance in conjunction with intensity.

$\boxed{\text{Teff High}}$: Good for counts, but Saha Ioniz Balance:

$$\Rightarrow kT_{1/2} \approx |E_{\rm bind}| / \ln(n_Q/n)$$

$$n_Q \approx 8\times10^{25} T_7^{3/2} \qquad n_e \sim 6\times10^{22}$$

$$\ln\frac{n_Q}{n} \simeq 7 \Rightarrow kT_{1/2}({\rm Fe}) \approx 1.3\ {\rm keV}$$

$\Rightarrow$ Maybe Fe, but not C, O....

$\boxed{\text{Teff Low}}$: Low Count Rate, BUT Lots of atomic physics,

$$kT_{1/2}(^{16}{\rm O}) \simeq 0.2\ {\rm keV},\ T_{\rm eff} = 10^6 {\rm K}$$

[NS Transients].

1996A&A...315..141Z

148 V.E. Zavlin et al.: Model neutron star atmospheres with low magnetic fields. I

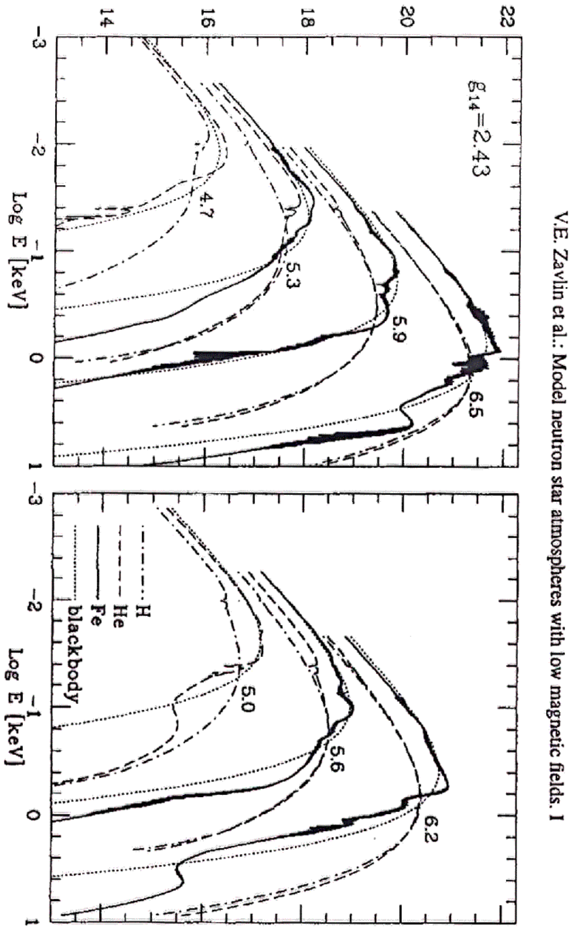

Fig. 5. Spectral fluxes of emergent radiation for hydrogen, helium and iron atmospheres with different values of log $T_{\rm eff}$ (nu curves). Dotted curves show the corresponding blackbody fluxes $\pi B_\nu(T_{\rm eff})$.

EXO 0748-676

- $P_{orb} \simeq 3.8$ hr LMXB
- D ~ 8-10 kpc
  $L_X \simeq 10^{36}$ erg/s but highly variable (EXOSAT Tr)
- Type I Bursts Seen at discovery ↳ Neutron Star

Cottam, Paerels + Mendez
Nature, 420, 51

- Calib/Commiss Data = 5×10^5 s
  [3.35×10^5 s RGS Data] ~ 6 days
- 28 Bursts Seen = 3200 s RGS
  (Only 1% of TIME)

Gottwald et al.: EXOSAT.

Burst Durations Range from 20 s → 150s in Hard Band.

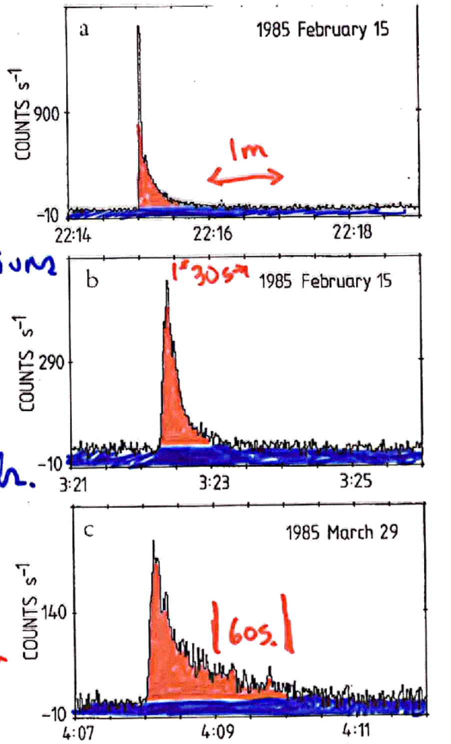

FIG. 3.—Light curves of representative "fast" (a) and (b) and "slow" (c) bursts in the energy range 1.5–15 keV (time resolution 1 s; horizontal: UT in hh:mm). Burst (a) showed radius expansion in its initial phase. The light curves are not dead-time corrected. Dead-time correction factors for the bursts peaks are 1.56 (a), 1.23 (b), and 1.13 (c).

For RGS,

$L_{peak} = 15 * L_{accr}$

Peak Ct = 9 c/s

Bursts limited 48 → 128 sec.

They split each burst in 1/2 + summed

Bright Phase Spectrum (10^4 γ's)

Decline Phase "

Cottam, Paerels + Mendez '02

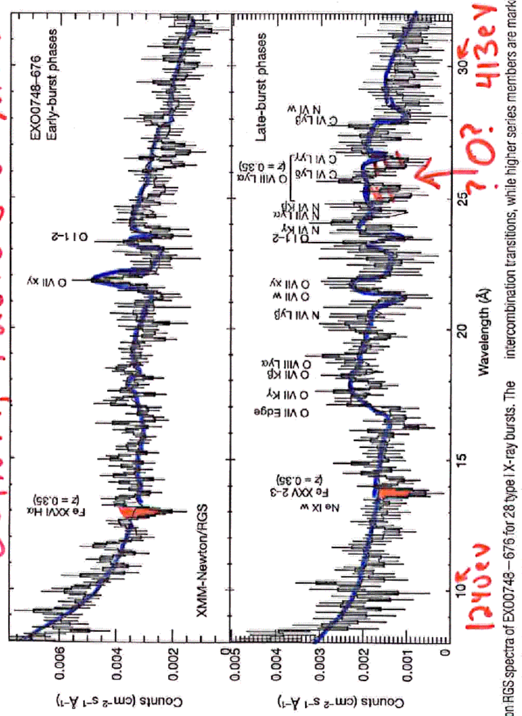

— Empirical Continuum + Absorption in photoion. Circumstell. Material

$Z = \frac{\Delta\lambda}{\lambda} = 0.35$

Figure 1 The XMM-Newton RGS spectra of EXO0748−676 for 28 type I X-ray bursts. The background-subtracted flux spectra for the early and late phases of the bursts are shown in the top and bottom panels, respectively. The data are plotted as the black histograms, with 1 σ error bars derived from counting statistics. The red line is the empirical continuum, with additional O VII intercombination line emission, modulated by absorption in photoionized circumstellar material. Red labels show the positions of the most prominent discrete absorption lines from the circumstellar medium; in the He-like spectra, 'w' signifies the $n = 1$–2 resonance transition, 'xy' the (unresolved) $n = 1$–2 intercombination transitions, while higher series members are marked 'Kβ,γ', and so on. Column densities in ions other than O VII have been normalized to the absorption measured in O VII, assuming an ionization parameter $\xi = 10$, and solar abundances. The N VII Lyα line at 24.78 Å is overpredicted, indicating a subsolar N/O abundance ratio. Black labels indicate the interstellar O 1s–2p absorption line. Blue labels indicate the photospheric absorption lines in Fe XXVI, Fe XXV and O VIII, at a redshift $z = 0.35$. The data and models have been rebinned to $\Delta\lambda = 0.124$ Å, which is about 2.5 times larger than the RGS instrument resolution.

52

© 2002 Nature Publishing Group

NATURE | VOL 420 | 7 NOVEMBER 2002 | www.nature.com/nature

$$\Rightarrow \quad R = 4.43\,\frac{GM}{c^2}$$

so $R \lesssim 6M$,

NS is inside last stable orbit.

$$R = 9.2\,\mathrm{km}\left(\frac{M}{1.4M_\odot}\right)$$

But M is NOT measured.

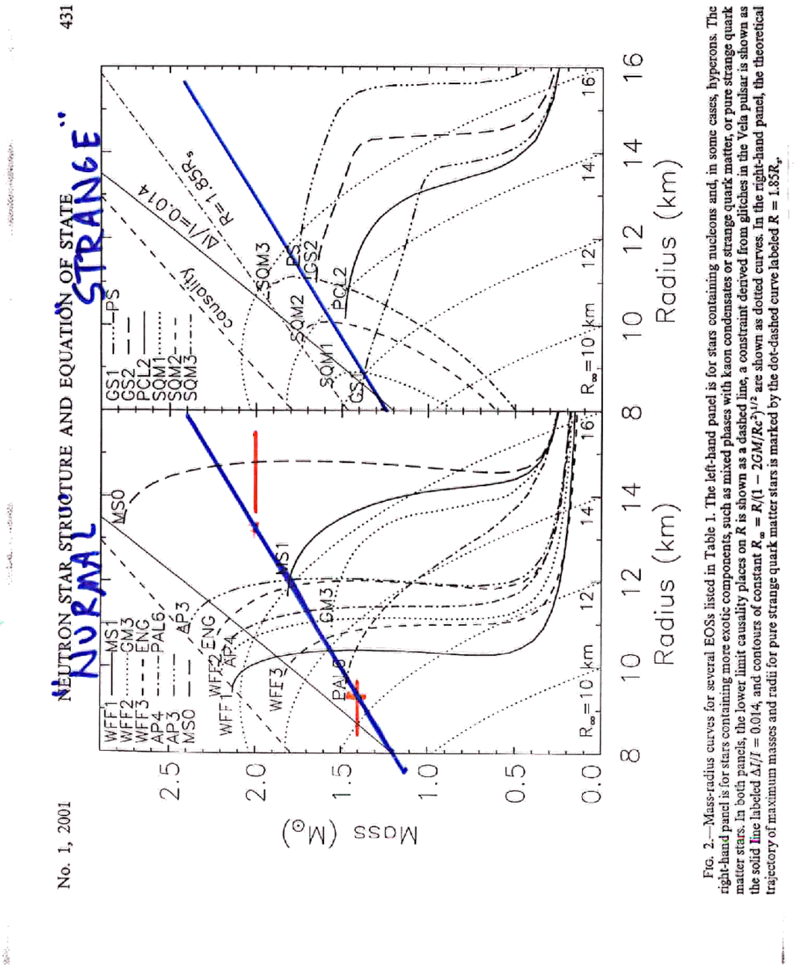

No. 1, 2001 NEUTRON STAR STRUCTURE AND EQUATION OF STATE 431

FIG. 2.—Mass-radius curves for several EOSs listed in Table 1. The left-hand panel is for stars containing nucleons and, in some cases, hyperons. The right-hand panel is for stars containing more exotic components, such as mixed phases with kaon condensates or strange quark matter, or pure strange quark matter stars. In both panels, the lower limit causality places on R is shown as a dashed line, a constraint derived from glitches in the Vela pulsar is shown as the solid line labeled $\Delta I/I = 0.014$, and contours of constant $R_\infty = R/(1 - 2GM/Rc^2)^{1/2}$ are shown as dotted curves. In the right-hand panel, the theoretical trajectory of maximum masses and radii for pure strange quark matter stars is marked by the dot-dashed curve labeled $R = 1.85R_s$.

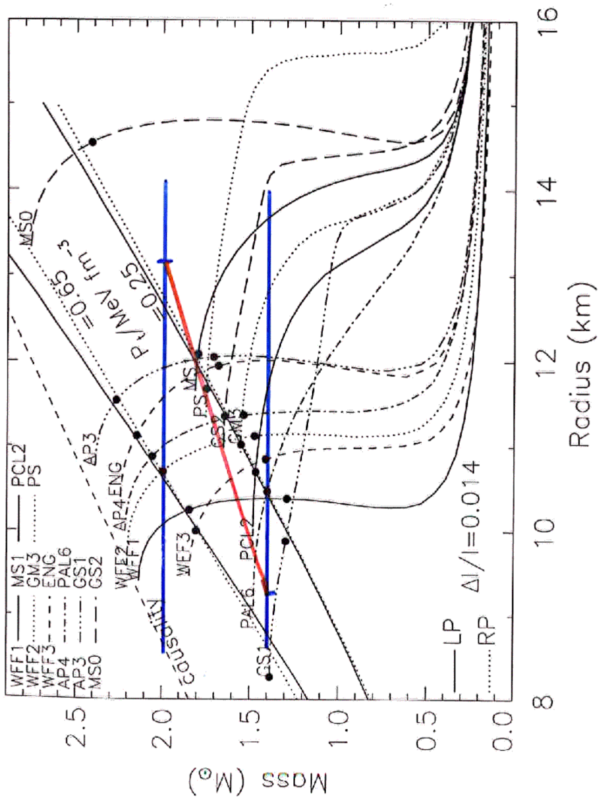

FIG. 7.—Mass-radius curves for selected EOSs from Table 1, comparing theoretical contours of $\Delta I/I = 0.014$ from approximations developed in this paper, labeled "LP," and from Ravenhall & Pethick (1994), labeled "RP," to numerical results (*filled circles*). Two values of P_t, the transition pressure demarking the crust's inner boundary, which bracket estimates in the literature, are employed. The region to the left of the $P_t = 0.65$ MeV fm^{-3} curve is forbidden if Vela glitches are due to angular momentum transfers between the crust and core, as discussed in Link et al. (1999). For comparison, the region excluded by causality alone lies to the left of the dashed curve labeled "causality" as determined by Lattimer et al. (1990) and Glendenning (1992).

Initial Theoretical Work

Bildsten, Chang & Paerels.
'03.

- Fe unlikely from Burning!
  - Entropy in Burning Layer Lower than Photosphere!

$$S \propto \frac{k}{m_p \mu} \ln\left(\frac{T^{5/2}}{P}\right)$$ (Joss '77)

Photosphere $\frac{(10^7)^{5/2}}{10^{14}} \simeq 3000$

Burning $\frac{(10^9)^{5/2}}{10^{23}} \simeq 0.3$

- Fe unlikely residual from Turned off Accretion

$V_{dr} \approx 1 \frac{cm}{s} \frac{T_7^{3/2}}{g} \Rightarrow$ 1 sec to fall beneath Photosphere

$\Rightarrow$ Fe likely from Accretion!

- Evidence in other bursters that accretion continues during burst + these bursts have $L < L_{Edd}$

So, presume same rate

$$\dot{M} \gtrsim 2 \times 10^{-10} M_\odot/yr$$

- Integrate last stable orbit $\Rightarrow$ to NS surface (Piro)

$$\sin\theta = 0.1 \qquad E = 200\text{-}300 \frac{\text{MeV}}{\text{nucl.}}$$

Since some J might be lost in accretion gap, $\sin\theta \gtrsim 0.1 \ldots$

- What is Fe's fate for $f_i = \left.\frac{n_{Fe}}{n_p}\right|_{\text{beam}} = 3 \times 10^{-5}$?

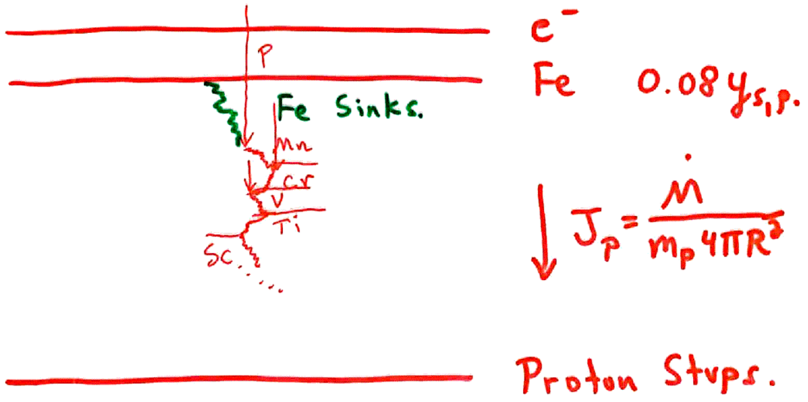

- While sinking, Fe is spalled by protons ($\sigma_D = 600$ mb)

$$\Rightarrow t_{dest} = \frac{1}{\sigma_D J_p} = 2.8\,\text{ms}\left(\frac{10^3}{\dot{m}}\right),$$

so when

$$\dot{M} > 4 \times 10^{-13} \frac{M_\odot}{yr} T_7^{3/2}$$

we have $t_{dest} < t_{sink}$

$\Rightarrow$ Fe Residence Time Set by Nuclear Physics!

⇒ As long as $\dot{M}$ during burst is > 1% before the burst then nuclear physics dominates:

Steady State

$$\text{Fe} \quad \underbrace{\dot{N}_{Fe}}_{\substack{\uparrow \\ \text{Changing Column} \left(\frac{\#}{cm^2 \cdot s}\right)}} = \underbrace{J_p f_i}_{\substack{\uparrow \\ \text{Accretion Deposition}}} - \underbrace{\sigma_D N_{Fe} J_p}_{\substack{\uparrow \\ \text{Destruction by Protons.}}}$$

Steady State:

$$\Rightarrow \quad N_{Fe} = \frac{f_i}{\sigma_D} = 4 \times 10^{19}\ cm^{-2}$$

! Independent of $\dot{M}$!

For all other Species of Cascade

$$\text{e.g.} \quad \dot{N}_{Cr} = \sum_{j>Cr} N_j J_p \sigma_D - \sum N_{Cr} J_p \sigma_D .$$

Bildsten, Chang & Paerels

Table 1. Heavy Element Abundances and Atomic Features

	E_e [keV(redsh)]	$\tau_{e,max}$	N_i/N_{Fe}	EW_e [eV]	$kT_{1/2}$ [keV]	$W_{H\alpha}$ [eV]
Fe	9.279(6.87)	0.32	1.00	277	1.12	7.4
Mn	8.573(6.35)	0.18	0.36	66	1.05	4.6
Cr	7.897(5.85)	0.26	0.48	56	0.99	4.5
V	7.248(5.37)	0.26	0.43	32	0.93	3.1
Ti	6.627(4.91)	0.31	0.48	22	0.86	2.3
Sc	6.035(4.47)	0.41	0.58	17	0.81	1.8
Ca	5.471(4.05)	0.47	0.59	11	0.75	1.2
K	4.934(3.65)	0.48	0.55	7	0.69	0.7
Ar	4.427(3.28)	0.53	0.54	4	0.65	0.4

These elements should be Prevalent!

Future

- Likely that more observ. like that of Cottam et al. will occur/be approved
- We hope that observers now search for the previously unexpected edges/lines from Mn, Cr, V...., ⇒ richer possibilities for atomic features than just Fe.
- INTEGRAL is searching for γ-ray lines now

∴ Neutron Star Spectroscopy is Now Beginning.